

Chimeric Peptides of Statherin and Osteopontin That Bind Hydroxyapatite and Mediate Cell Adhesion*

Received for publication, March 3, 2000
Published, JBC Papers in Press, March 20, 2000, DOI 10.1074/jbc.M001773200

Michele Gilbert‡, Wendy J. Shaw§, Joanna R. Long‡, Kjell Nelson‡, Gary P. Drobny§, Cecilia M. Giachelli‡, and Patrick S. Stayton‡¶

From the ‡Department of Bioengineering and §Department of Chemistry, University of Washington, Seattle, Washington 98195

Extracellular matrix proteins play key roles in controlling the activities of osteoblasts and osteoclasts in bone remodeling. These bone-specific extracellular matrix proteins contain amino acid sequences that mediate cell adhesion, and many of the bone-specific matrix proteins also contain acidic domains that interact with the mineral surface and may orient the signaling domains. Here we report a fusion peptide design that is based on this natural approach for the display of signaling peptide sequences at biomineral surfaces. Salivary statherin contains a 15-amino acid hydroxyapatite binding domain (N15) that is loosely helical in solution. To test whether N15 can serve to orient active peptide sequences on hydroxyapatite, the RGD and flanking residues from osteopontin were fused to the C terminus. The fusion peptides bound tightly to hydroxyapatite, and the N15-PGRGDS peptide mediated the dose-dependent adhesion of Mo α_v melanoma cells when immobilized on the hydroxyapatite surface. Experiments with an integrin-sorted Mo α_v subpopulation demonstrated that the $\alpha_v\beta_3$ integrin was the primary receptor target for the fusion peptide. Solid state NMR experiments showed that the RGD portion of the hydrated fusion peptide is highly dynamic on the hydroxyapatite surface. This fusion peptide framework may thus provide a straightforward design for immobilizing bioactive sequences on hydroxyapatite for biomaterials, tissue engineering, and vaccine applications.

hydroxyapatite (HAP)¹ growth (2). These proteins, such as statherin and histatin, directly modulate the nucleation and/or growth of calcium phosphate minerals. We have recently reported the first high resolution structural and dynamic studies of statherin peptides on HAP surfaces (5, 6), which have provided insight into how these peptides recognize crystal surfaces. Other biomineralization proteins contain acidic domains as part of a much larger architecture and set of functional domains. The primary function of many of these proteins is to mediate cellular function at the mineral interface. Because of their important role in hard tissue remodeling and healing, the biomineralization proteins have been of considerable interest in the biomaterials and tissue engineering fields. An important example in this group is osteopontin, which contains a polyaspartic acid domain, as well as cell interaction domains that include an Arg-Gly-Asp (RGD) integrin-binding sequence (7). Although there are neither solution nor surface adsorbed structural data available for osteopontin, it is likely that the polyacidic stretch is responsible for binding the protein to HAP, while orienting the cell interaction domains away from the mineral surface.

There are a number of technologies where design principles from these naturally occurring acidic proteins and peptides could prove useful. For biomaterial, tissue engineering, or biosensor applications, the acidic domain could be used as an anchor and coating on inorganic surfaces to present accessible, bioactive peptides in favorable orientations. A similar principle could be useful in vaccine development, where antigenic peptides and proteins need to be presented in accessible and favorable orientations from inorganic surfaces (8, 9). In order to develop a peptide adaptor system for orienting bioactive peptides on HAP surfaces, we have utilized the HAP binding domain from the salivary protein statherin. The N-terminal residues of statherin are necessary for binding of the protein to mineral surfaces and for the inhibition of secondary crystallization (10). Solution state secondary structure analyses have suggested that this sequence has a propensity for amphipathic helix formation, which has been confirmed for the surface adsorbed peptide by recent solid state NMR studies (5). These NMR studies have demonstrated that the C-terminal portion of the peptide is dynamic and weakly interacting with the surface, suggesting that this acidic domain may have been de-

Polyacidic regions are a common motif in proteins that interact with inorganic ions and mineral surfaces (1). The acidic domains directly mediate protein binding to hydroxyapatite, and a number of general electrostatic and direct lattice matching models have been proposed (2–4). Despite the commonality of the acidic domains, the proteins involved in biomineralization processes vary widely in their properties and biological roles. The small polypeptides found in salivary fluids have been extensively studied in the context of their physical effects on

* This work was supported by National Institutes of Health NIDR Grant DE 12554-01, National Science Foundation University of Washington Engineered Biomaterials Engineering Research Center Grant EEC-9529161, a Whitaker Foundation graduate fellowship (to M. G.), and the Office of Science, Office of Basic Energy Sciences, Department of Energy, through an Associated Western Universities graduate fellowship (to W. J. S). The costs of publication of this article were defrayed in part by the payment of page charges. This article must therefore be hereby marked "advertisement" in accordance with 18 U.S.C. Section 1734 solely to indicate this fact.

¶To whom correspondence should be addressed: Dept. of Bioengineering, Box 352125, University of Washington, Seattle, WA 98195. Tel.: 206-685-8148; Fax: 206-685-8256; E-mail: stayton@u.washington.edu.

¹ The abbreviations used are: HAP, hydroxyapatite; N15, N-terminal 15 residues of human salivary statherin; N15-PGRGDS, N-terminal 15 residues of human salivary statherin with PGRGDS fused to the C terminus; N15-PGRGES, N-terminal 15 residues of human salivary statherin with PGRGES fused to the C terminus; 30N OPN, N-terminal fragment of recombinant human osteopontin after thrombin cleavage; BSP II, bone sialoprotein II; Fmoc, 9-fluorenylmethoxycarbonyl; PBS, phosphate-buffered saline; DMEM, Dulbecco's modified Eagle's medium; BSA, bovine serum albumin fraction V.

signed by nature to adhere to HAP, leaving the rest of the protein mobile and exposed on the crystal surface. This exposure of the remainder of the surface-bound protein could explain its selective ability to bind the protein fibronectin on bacterial membranes when immobilized (11). We have thus

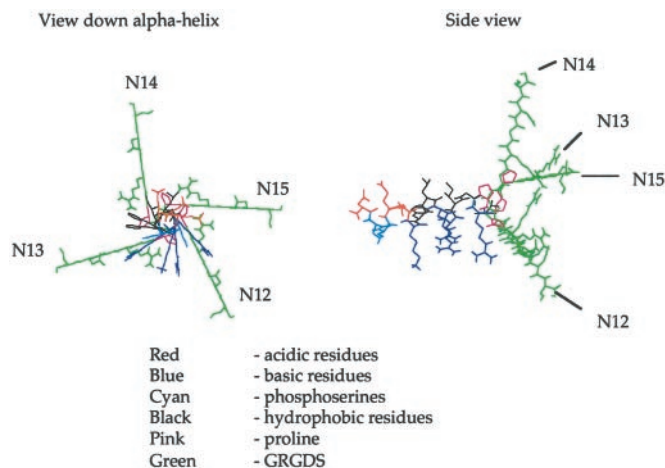


FIG. 1. A view down the central axis of the modeled statherin α -helix which shows the amphipathic nature of the peptide, and a side view of different length statherin N-terminal peptides fused to a PGRGDS sequence which depicts the potential orientations of the cell binding sequence relative to the surface as a function of the length of the mineral binding sequence.

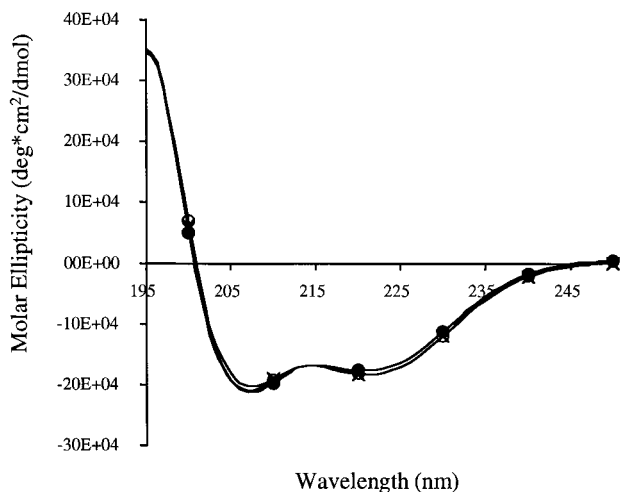
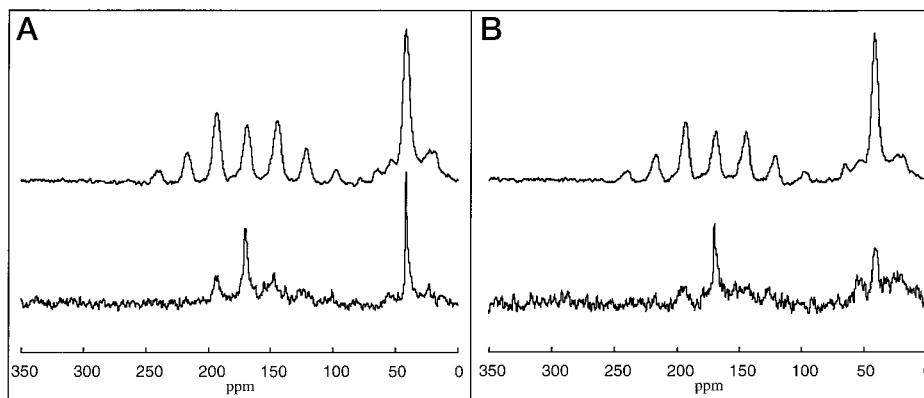


FIG. 2. Circular dichroism spectra of N15 (●) and the fusion peptides N15-PGRGDS (○) and N15-PGRGES (×) at $200 \mu\text{M}$ in IX PBS, pH 7.3. The spectra demonstrate that the three peptides all display loosely helical structure and that there are no significant differences between the three peptides.

FIG. 3. Solid state NMR characterization of HAP-adsorbed N15-PGRGDS (a) and N15-PGRGES (b) in lyophilized (top) and hydrated (bottom) states. Both spectra represent 10,240 scans. The hydrated spectrum displays a significant loss of signal intensity (and thus cross-polarization efficiency) and narrowing of the carbonyl chemical shift anisotropy (~ 170 ppm), indicating there are large amplitude dynamics at the labeled C-terminal region of the fusion peptides.



designed a fusion peptide between the N15 peptide of statherin (DpSpSEEKFLRRIGRFG, where pS stands for phosphoserine) and the RGD integrin binding domain from osteopontin. We report here the functional characterization of this minimized fusion peptide that contains a HAP recognition sequence and a cell interaction sequence, inspired by the naturally occurring design of osteopontin and statherin.

EXPERIMENTAL PROCEDURES

Secondary Structure Predictions for Acidic Repeat Domains in Natural Proteins—Chou-Fasman and Garnier-Osguthorpe-Robson algorithms were used with the GCG program (Genetics Computer Group, Madison, WI) PredictPeptide to predict the secondary structure of acidic domains from several biomineralization proteins. The predicted α -helical regions of these proteins were then mapped onto helical wheels using the program HelicalWheel to determine if the helix of any of the proteins exhibited amphipathicity. This procedure was performed on osteopontin, osteonectin, bone sialoprotein II (BSP II), and statherin (for which amphipathicity has been previously predicted; Ref. 12), which are all known to adhere to hydroxyapatite.

Synthesis and Characterization of Fusion Peptides—The N15-PGRGDS, N15-PGRGES, and N15 peptides were synthesized using standard Fmoc solid phase synthesis. Fmoc-protected amino acids, including protected phosphoserine (Fmoc-Ser(PO(OBzl)OH)-OH), and preloaded resins were purchased from Novabiochem and Advanced Chemtech. [^{13}C]-Carbon-labeled glycine and [^{13}C]-carbonyl-labeled glycine were purchased from Cambridge Isotope Laboratories and protected with Fmoc using standard protocols. The labeling scheme is as follows: DpSpSEEKFLRRIG* $\text{RFLPGRG}^{**}(\text{D/E})\text{S}$, where G* is labeled at the α -carbon, G** is labeled at the carbonyl carbon, and pS stands for phosphoserine. The isotopically labeled peptides were synthesized by United Biochemical Research, Inc. (Seattle, WA). The three non-isotopically labeled peptides were synthesized on an automated Applied Biosystems 433A peptide synthesizer. All couplings were done in 4-fold excess of protected amino acids using the 2-(1H-benzotriazole-1-yl)-1,1,3,3-tetramethyluronium hexafluorophosphate/*N*-hydroxybenzotriazole coupling method in *N*-methylpyrrolidine. After each coupling, unreacted peptides were acetylated to terminate subsequent synthesis.

The peptides were cleaved from the resin and deprotected in 82.5% trifluoroacetic acid, 5% phenol, 5% thioanisole, 2.5% ethanedithiol, and 5% water. After allowing the reaction to proceed with gentle mixing for 4 h, solutions were filtered and concentrated to approximately 5 ml. The trifluoroacetic acid/peptide solutions were then added dropwise to cold *t*-butyl methyl ether and washed. The precipitate was dried under nitrogen, dissolved in water, and purified using a Waters HPLC C-18 reverse phase column. Both the N15-PGRGDS and N15-PGRGES peptides were purified using a 20–40% acetonitrile, 0.1% trifluoroacetic acid gradient in water, and N15 was purified using a 10–40% acetonitrile, 0.1% trifluoroacetic acid gradient in water. Purified non-isotopically labeled peptides were lyophilized and analyzed using matrix-assisted laser desorption/ionization mass spectrometry to verify molecular weight and purity of the peptides. The isotopically labeled peptides were analyzed using electrospray ionization mass spectrometry to verify the incorporation of the isotopic labels.

Determination of Peptide Adsorption Isotherms on HAP—Concentrated stock solutions of N15, N15-PGRGDS, and N15-PGRGES in double-distilled H_2O were made, and the peptide concentration was

determined using amino acid analysis. The concentration *versus* fluorescence dependence was determined using 100 μl of serially diluted peptides in 1 ml of formaldehyde (Pierce) with excitation at 360 nm and emission at 445 nm on a Hitachi model F-4500 fluorescence spectrophotometer. The formaldehyde assay determines the number of primary amines present (two in each peptide). Various concentrations of peptide were added to 1 mg of ceramic HAP that had been autoclaved, and the peptide was adsorbed to the surface for 4 h at 37 °C. Samples without HAP were also made that contained the same volume of serially diluted peptide to serve as controls. Samples were performed in triplicate for each peptide concentration. After the incubation, the peptide concentrations in the supernatant were determined with the formaldehyde assay, and the peptide on the surface was determined by subtraction. The initial concentration was determined from the samples without HAP. Langmuir isotherms were plotted with the *C* values calculated from the depleted supernatant and the *Q* values determined by depletion using a Brunauer-Emmett-Teller method-measured surface area of 55 m^2/g (performed by Allison Campbell, Battelle Pacific Northwest Laboratory) for the Bio-Rad HAP.

Circular Dichroism and Solid State NMR Characterization of Struc-

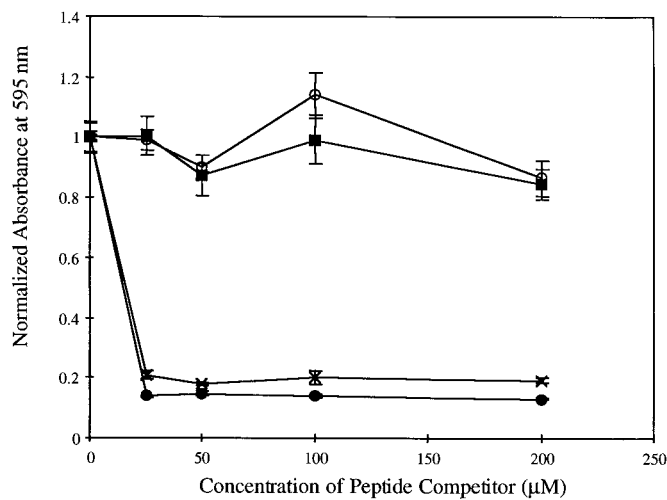
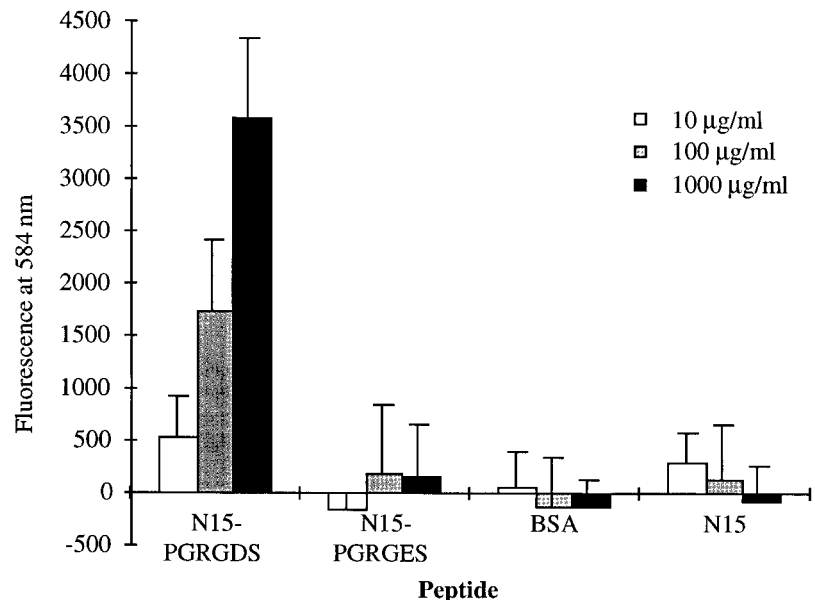


FIG. 4. **Determination of peptide specificity in cell recognition.** Competition studies were conducted to assess whether soluble GRGDSP (●), GRGESP (○), N15-PGRGDS (×), or N15-PGRGES (■) peptides could block $\text{Mo}\alpha_v$ cell binding to immobilized 30N OPN on non-tissue culture polystyrene wells. Values are expressed as the mean ($n = 9$) with each experiment repeated at least three times (*bars* represent the S.E.). In solution, the N15-PGRGDS peptide shows the same dose-dependent blocking of cell binding to the immobilized 30N OPN as the small linear peptide GRGDSP.

FIG. 5. **Dose-dependent binding and RGD specificity of $\text{Mo}\alpha_v$ cell binding to peptide-coated ceramic HAP beads.** Values are expressed as means ($n = 6$) with each experiment repeated two times, and *bars* represent the S.E. Analysis of variance was used to test if significant differences existed for dose dependence for each different HAP coating and also to determine significant differences in the effects of different coatings at the same initial concentration. Subsequently, the Student-Newman-Keuls analysis determined the level of significance.



ture and Dynamics—200 μM solutions of N15, N15-PGRGDS, and N15-PGRGES were made in 1 \times PBS (140 mM NaCl, 2.7 mM KCl, 10 mM Na_2HPO_4 , 1.8 mM KH_2PO_4 , pH 7.3). The circular dichroism spectra were recorded for each sample on an Aviv Circular Dichroism model 62ADS at 1-nm intervals using a quartz cell with path length 0.1 cm in the wavelength range of 195–250 nm. All spectra were corrected using the solvent spectra and represent the average of 10 scans.

^{13}C chemical shift spectra were taken using cross-polarization with magic angle spinning on a Chemagnetics CMX Infinity spectrometer operating at a ^{13}C frequency of 125.72 MHz using a Chemagnetics doubly resonant magic angle spinning probe. These experiments employed a ^1H 90° pulsewidth of 7.5 ms, followed by a contact time of 1.5 ms and a spinning speed of 3003 Hz. The surface-adsorbed samples were signal-averaged for 10240 scans. The chemical shifts were referenced externally to hexamethyl benzene. Samples were prepared by adsorbing 2 mM peptide in modified PBS (100 mM NaCl, 40 mM KCl, 4.3 mM Na_2HPO_4 , 1.4 mM KH_2PO_4) to hydroxyapatite crystals for 4 h, followed by repeated washes with buffer. The resulting slurry was then transferred to the rotor and packed by repeatedly spinning the sample and removing excess solution, leaving the final surface-adsorbed peptide in the bulk hydrated state. To facilitate direct comparisons between hydrated and lyophilized samples, the hydrated spectra were characterized first, with the same sample being subsequently frozen and lyophilized in the rotor prior to acquisition of the lyophilized spectra.

Cell Adhesion Assays—The $\text{Mo}\alpha_v$ cell line is a human melanoma cell line derived from the M21 cell line as described previously (13, 14). The $\text{Mo}\alpha_v$ cell line has been determined to express high levels of the $\alpha_v\beta_3$ integrin. The cells were grown on tissue culture polystyrene in Dulbecco's modified Eagle's medium (DMEM) supplemented with 10% fetal calf serum and 1% penicillin/streptomycin at 37 °C and 5% CO_2 until 80–90% confluence. Adhesion of melanoma cells to recombinant human 30N osteopontin-coated 96-well microtiter dishes was performed as described previously (14). Briefly, 200 μl of 200 nM recombinant 30N osteopontin was coated into the wells of non-tissue culture 96-well microtiter dishes (Maxisorp; Nunc Inc., Naperville, IL). The 30N OPN was allowed to bind for 1 h at 37 °C, and then the wells were aspirated. The wells were blocked with the addition of 200 μl of 10 mg/ml BSA in 1 \times PBS for 1 h at 37 °C and then washed three times with Dulbecco's 1 \times PBS + Ca^{2+} + Mg^{2+} .

The melanoma cells were detached from the tissue culture flasks with Versene (Life Technologies, Inc.) and then washed in DMEM, 10 mM HEPES, 1 mg/ml BSA. The cells were resuspended in the DMEM, 10 mM HEPES, 1 mg/ml BSA and pre-incubated with varying concentrations of the peptides GRGDSP, GRGESP, N15-PGRGDS, or N15-PGRGES at 37 °C and 5% CO_2 for 15 min. After incubation, the cells were added at a level of 200,000 cells/well and allowed to bind for 1 h, at which point the media and non-adherent cells were aspirated off, the wells were washed with Dulbecco's 1 \times PBS, and then the adherent cells were fixed with 4% paraformaldehyde, stained with 0.5% toluidine blue in 4% paraformaldehyde, and solubilized with 1% SDS. The absorbance at 595 nm was measured, which correlates to the number of adherent

cells (15).

Adhesion of Cells to Peptide-coated Hydroxyapatite—Adhesion of melanoma cells to peptide-coated hydroxyapatite was studied using a modified protocol from Fujisawa *et al.* (16). Varying concentrations of N15, N15-PGRGDS, N15-PGRGES, and BSA were made using sterile 1× PBS. 3 mg of autoclaved, 80 μm diameter, ceramic hydroxyapatite (Bio-Rad) were incubated with 200 μl of peptide solution at 4 °C overnight. The peptide solution was removed, and the HAP was washed with 100 μl of sterile double-distilled H₂O. Moα_v and Mo human melanoma cells were grown to subconfluence, detached using Versene, washed, and resuspended in DMEM, 10 mM HEPES, 1 mg/ml BSA at a final cell density of 100,000 cells/100 μl. 200 μl of these cells were added to each Eppendorf tube containing the peptide-coated HAP. The cells were incubated for 1 h at 37 °C and 5% CO₂, and the supernatant was aspirated off.

150 μl of DMEM, 10 mM HEPES, 1 mg/ml BSA with 30% Ficoll (Amersham Pharmacia Biotech) was then added to each tube, and the tubes were centrifuged at 2000 rpm for 10 min at 22 °C. The unattached cells segregated to the Ficoll layer, whereas the cells bound to peptide-coated HAP were pelleted. The supernatant containing unattached cells was carefully removed and 200 μl of DMEM, 10 mM HEPES, 1 mg/ml BSA, and 20 μl of alamarBlue (BIOSOURCE International, Camarillo, CA) were added back to the tubes. The cells were then incubated for 2.75 h at 37 °C. The number of cells adhered was determined by measuring the fluorescence of the supernatant at 584 nm. The fluorescence measurements were performed on a Hitachi model F-4500 fluorescence spectrophotometer. Significance was calculated using the Student-Newman-Keuls test. Previous experiments showed that the HAP and peptides alone do not reduce the alamarBlue. For competition assays between adsorbed N15-PGRGDS and soluble linear GRG(D/E)SP, the standard cell adhesion to peptide-coated HAP assay was used with minor modifications. First, 1 mg/ml N15-PGRGDS was adsorbed to the HAP for all samples. The cells were subsequently pre-incubated with varying concentrations (0–200 μM) of GRGDSP or GRGESP for 15 min at 37 °C and 5% CO₂, and then added to the N15-PGRGDS-coated HAP. All other portions of the protocol remained the same.

RESULTS AND DISCUSSION

Design of the Statherin-Osteopontin Fusion Peptide—Proteolysis studies have determined that the acidic domains of various biomineralization proteins are necessary for HAP binding and control of mineral formation (2, 4, 17, 18). In order to design an HAP adaptor that could potentially display bioactive fusion peptide sequences, we searched for an amphiphilic helical sequence that could orient the adaptor on the HAP surface. Only statherin exhibited helical amphipathicity. The predicted amphipathicity of the N-terminal portion of statherin has been

noted previously by Ramasubbu *et al.* (12) when studying the lubrication properties of statherin, and Raj *et al.* (10) while studying the mineral inhibition effects of the N15 portion of statherin. The other proteins analyzed all contain several functional domains and are much larger than statherin (BSP II, 59 kDa; OPN, 80 kDa; osteonectin, 32 kDa *versus* 5.3 kDa for statherin).

The N terminus of statherin has been shown to be important for binding to HAP (10). Molecular models of the N-terminal portion of statherin fused to an RGD-containing sequence were constructed using PSSHOW (E. Swanson, Seattle, WA). The statherin residues predicted to be helical by secondary structure predictions were modeled with α-helix backbone torsional angles. A proline residue was then added and followed by the sequence GRGDS in an extended structure. The statherin portion of the peptide was modeled using the first 12, 13, 14, or 15 residues of statherin (N12, N13, N14, and N15, respectively). These statherin peptides were “fused” to the sequence PGRGDS to determine which direction the cell binding domain would face relative to the plane defined by the N-terminal serines 2 and 3 of statherin, assuming that the phosphorylated side chains were interacting with the hydroxyapatite surface. The proline was fused to the N15 sequence using the standard Ponder and Richards rotamer angles. The N15 peptide was subsequently chosen as the adaptor sequence, because these simple steric models suggested that the PGRGDS sequence would be directed toward the crystal surface with N12 or N13 peptides (Fig. 1). The proline was added at the junction to promote the turn of the sequence away from the surface.

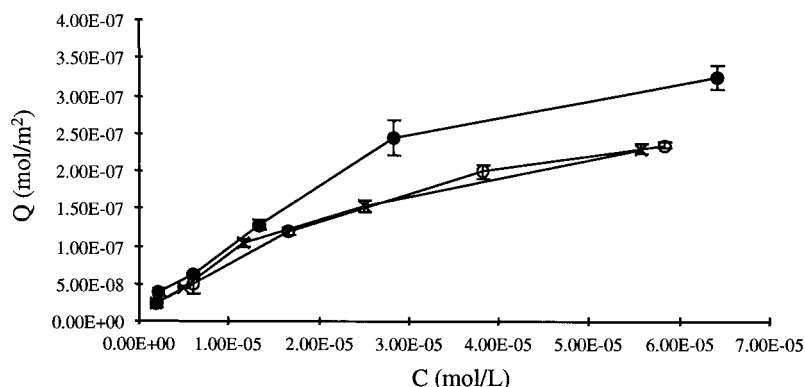
Characterization of Peptide Structure and Dynamics—Statherin’s N-terminal domain exhibits some α-helicity in solution as determined by circular dichroism (10). The circular dichroism spectra for N15, N15-PGRGDS, and N15-PGRGES are shown in Fig. 2. The results suggest that the addition of the cell binding sequences do not significantly alter the structure of the N15 peptide in solution. Recent solid state NMR characterization has suggested that the acidic pentapeptide portion of the N15 peptide has a random coil structure when adsorbed to HAP, whereas the middle and C-terminal portion of N15 display significant helical content (5). Dynamics studies of the hydrated peptide on the HAP surface have shown that the acidic sequence is tightly bound to HAP, whereas the C terminus is weakly bound and highly mobile on the surface.² Taken together, the NMR and sequence analyses thus suggested that the N-terminal statherin peptide could direct tight and oriented binding to HAP, while allowing display of a relatively mobile sequence at the C terminus to which other sequences could be added.

To test whether the C terminus of the fusion peptides are still dynamic on the HAP surface, despite the presence of the new C-terminal acidic residue (Asp or Glu), solid state NMR

TABLE I
Langmuir isotherm parameters calculated for N15 and N15 fusion peptides adsorbed to 55 m²/g surface area HAP

| | N | Standard deviation | K | Standard deviation |
|------------|--|--|--|--|
| | <i>mol/m</i> ² (× 10 ⁻⁷) | <i>mol/m</i> ² (× 10 ⁻⁸) | <i>liter/mol</i> (× 10 ⁴) | <i>liter/mol</i> (× 10 ³) |
| N15 | 4.65 | 5.06 | 3.30 | 5.24 |
| N15-PGRGDS | 3.62 | 0.594 | 3.00 | 2.02 |
| N15-PGRGES | 3.71 | 2.24 | 3.45 | 3.16 |

FIG. 6. Adsorption isotherm for the binding of N15 (●), N15-PGRGDS (○) and N15-PGRGES (×) onto 80-μm diameter ceramic Bio-Rad HAP. N and K values were calculated from regression of C versus C/Q. The Langmuir model analysis demonstrated that K was not significantly different for the three peptides, whereas N was significantly higher for N15 (*p* < 0.01).



² Shaw, W. J. (2000) *J. Am. Chem. Soc.*, in press.

was used to probe the dynamics of the peptides bound to HAP. The chemical shift tensors (19) are very sensitive to molecular dynamics and electronic structure (20), and thus reflect how tightly bound that portion of the peptide is to HAP. As mobility increases, the width of the spinning sideband pattern (anisotropy) becomes more narrow. As Fig. 3 demonstrates, both the N15-PGRGDS and N15-PGRGES peptides at the G_{19} carbonyl-labeled positions exhibit significant narrowing of the anisotropy (by a factor of 2–3). There is also a loss of signal intensity for the hydrated samples, indicating poor cross-polarization efficiency. Taken together, these results directly demonstrate that there is large amplitude motion at the C terminus present in both hydrated peptides on HAP.

The N15-PGRGDS Peptide Mediates Specific RGD-dependent Cell Adhesion—Competition assays were performed in solution to ensure that the RGD segment was accessible to cell surface integrins in the fusion peptide. The N15-PGRGDS fusion peptide inhibited $Mo\alpha_v$ melanoma cell binding to immobilized 30N OPN in the same dose-dependent manner as the small linear peptide GRGDSP (Fig. 4). This demonstrates that the RGD domain is accessible within the context of the N15 fusion sequence and sterically similar to the free GRGDSP peptide. These results also demonstrate that the high negative charge of the N15 sequence does not inhibit binding to cell surface receptors. The cell binding was RGD-dependent and not a function of the N15 sequence, as the control N15-PGRGES peptide did not inhibit cell binding to the immobilized 30N OPN.

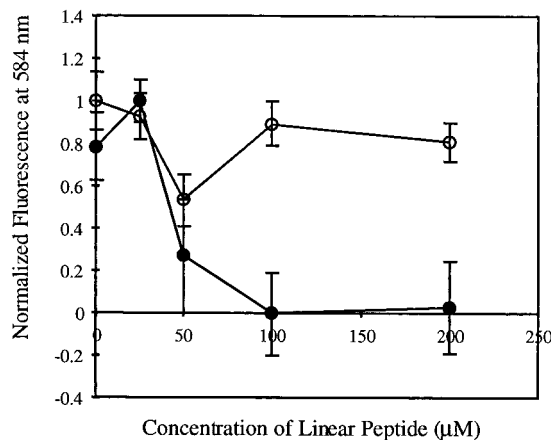
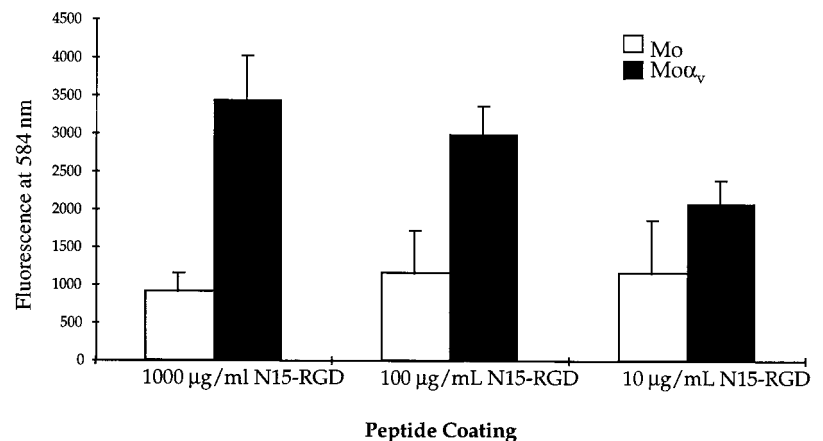


FIG. 7. **RGD dependence of cell binding to the immobilized fusion peptide.** $Mo\alpha_v$ cells were preincubated with soluble competitors GRGDSP (●) or GRGESP (○) before allowing the cells to bind to N15-PGRGDS-coated Bio-Rad ceramic HAP. The soluble GRGDSP peptide did inhibit binding of the cells to the immobilized N15-PGRGDS whereas the GRGESP peptide has no appreciable effect on cell binding.

FIG. 8. **Integrin specificity of cell binding to N15-PGRGDS-coated ceramic Bio-Rad HAP beads.** Cell binding was compared between $\alpha_v\beta_3$ -deficient Mo cells and $\alpha_v\beta_3$ -containing $Mo\alpha_v$ cells. Values are expressed as the mean ($n = 6$) with each experiment repeated at least two times. At each coverage level, the significance of the binding differences was tested using a standard two-tailed Student's t test. At 1000 $\mu\text{g}/\text{ml}$, the difference was significant at a level of $p < 0.001$, and at 100 $\mu\text{g}/\text{ml}$, the significance was $p < 0.002$, whereas there was much lower significance at 10 $\mu\text{g}/\text{ml}$ with $p < 0.1$.



The RGD domain of the N15-PGRGDS is also accessible when the peptide is adsorbed onto HAP, where it directs $Mo\alpha_v$ cell adhesion to the ceramic surface (Fig. 5). Prior to determining dose dependence values for cell adhesion, adsorption isotherms were determined for the N15-PGRGDS, N15-PGRGES, and N15 peptides. The results were analyzed with a Langmuir binding model. There were no significant differences in N or K values between the RGD- and RGE-containing peptides. The N value is slightly higher for N15 compared with the RGD and RGE fusion peptides, consistent with the smaller size of this peptide (Table I). These isotherms were used to select three concentration values of N15-PGRGDS for determining the dose response. The 1 mg/ml solution value corresponds to a surface coverage at the adsorption plateau maximum, whereas the 100 $\mu\text{g}/\text{ml}$ and 10 $\mu\text{g}/\text{ml}$ correspond to a range of sub-monolayer coverages for the three peptides (Fig. 6). Dose-dependent binding of the $Mo\alpha_v$ cells to the N15-PGRGDS-coated HAP was observed over this range of surface coverages. Controls with N15-PGRGES or BSA demonstrated that cell binding was RGD-dependent. Competition assays provided additional evidence that the RGD domain was mediating melanoma cell adhesion. The $Mo\alpha_v$ cell binding to N15-PGRGDS immobilized on HAP could be competitively reduced with the addition of the small linear peptide GRGDSP (Fig. 7). As expected, the GRGESP peptide did not inhibit cell binding. A trend of decreasing nonspecific cell adsorption with increasing amounts of N15 adsorbed to HAP was also found. This trend suggests that the N15 peptide is masking sites on HAP that promote nonspecific cell interactions. A similar effect with renal cells has been reported, where anionic peptides (uropontin, nephrocalcin, etc.) block nonspecific adsorption of cells onto the positively charged HAP surface (21).

Integrin Specificity of Melanoma Cell Binding to N15-PGRGDS-coated Hydroxyapatite—Because monoclonal antibodies bind nonspecifically to the HAP ceramic, the selective blocking of specific integrins on the $Mo\alpha_v$ cells could not be used to determine which receptors were involved in recognition of the immobilized N15-PGRGDS peptide. In order to provide insight into the predominant integrin involvement, a sorted melanoma cell line that differs in expressed integrin populations was therefore utilized. The Mo line displays low expression of the $\alpha_v\beta_3$ integrin and the $Mo\alpha_v$ line expresses high levels of the $\alpha_v\beta_3$ integrin. The levels of other integrin receptor expression was similar for both cell lines as determined by fluorescence-activated cell sorting analysis (14). An alamarBlue titration analysis was performed on these cell lines to confirm that they display equivalent capabilities for dye reduction, and thus this technique can be used to directly compare the level of cell binding. The $Mo\alpha_v$ cells bind at a significantly higher level than the Mo cells for all initial concentrations of

peptide except 10 $\mu\text{g/ml}$ (Fig. 8). The Mo cells do bind to the N15-PGRGDS at reduced levels, potentially through $\alpha_9\beta_1$, which is known to recognize the RGD sequence (14), although they do not display any concentration dependence of binding within this range.

Conclusion—A fusion peptide was designed that combines the cell recognition sequence from osteopontin and the HAP recognition sequence from the salivary protein statherin. The N15-PGRGDS fusion protein functions as a minimized peptide that binds tightly to HAP and directs integrin-dependent cell adhesion at ceramic surfaces. The N15 portion of the peptide has been previously shown to be helical at the HAP surface, with tight association to HAP at the acidic N terminus and weaker interactions at the C-terminal region that result in large amplitude dynamics.² The RGD region of the fusion peptide is also highly dynamic on HAP, suggesting that the N-terminal portion of the fusion peptide tethers it to the HAP surface while the C-terminal RGD fusion domain remains accessible for integrin receptor engagement. This fusion peptide design may thus serve as a general route for immobilizing a variety of bioactive sequences to calcium phosphate surfaces for applications in biomaterial coatings, tissue engineering, and vaccine delivery.

Acknowledgments—Some of the solid state NMR portion of this research was performed in the Environmental Molecular Sciences Laboratory (a national scientific user facility sponsored by the Department of Energy (DOE) Office of Biological and Environmental Research) located at Pacific Northwest National Laboratory, operated by Battelle for the DOE.

REFERENCES

- Gorski, J. P. (1992) *Calcif. Tissue Int.* **50**, 391–396
- Johnsson, M., Levine, M. J., and Nancollas, G. H. (1993) *Crit. Rev. Oral Biol. Med.* **4**, 371–378
- Boskey, A. L. (1995) *Ann. N. Y. Acad. Sci.* **760**, 249–256
- Fujisawa, R., and Kuboki, Y. (1991) *Biochim. Biophys. Acta* **1075**, 56–60
- Shaw, W. J., Long, J. R., Dindot, J. R., Campbell, A. A., Stayton, P. S., and Drobny, G. P. (2000) *J. Am. Chem. Soc.* **122**, 1709–1716
- Long, J. R., Dindot, J. L., Zebroski, H., Kiihne, S., Clark, R. H., Campbell, A. A., Stayton, P. S., and Drobny, G. P. (1998) *Proc. Natl. Acad. Sci. U. S. A.* **95**, 12083–12087
- Butler, W. T. (1995) *Ann. N. Y. Acad. Sci.* **760**, 6–11
- Sood, A., Venugopalan, P., Mysore, N., and Vyas, S. P. (1998) *Indian J. Exp. Biol.* **36**, 849–861
- Beekman, N. J., Schaaper, W. M., Turkstra, J. A., and Meloen, R. H. (1999) *Vaccine* **17**, 2043–2050
- Raj, P. A., Johnsson, M., Levine, M. J., and Nancollas, G. H. (1992) *J. Biol. Chem.* **267**, 5968–5976
- Amano, A., Kataoka, K., Raj, P. A., Genco, R. J., and Shizukuishi, S. (1996) *Infect. Immun.* **64**, 4249–4254
- Ramasubbu, N., Thomas, L. M., Bhandary, K. K., and Levine, M. J. (1993) *Crit. Rev. Oral Biol. Med.* **4**, 363–370
- Chen, Y. P., O'Toole, T. E., Leong, L., Liu, B. Q., Diaz-Gonzalez, F., and Ginsberg, M. H. (1995) *Blood* **86**, 2606–2615
- Smith, L. L., Cheung, H. K., Ling, L. E., Chen, J., Sheppard, D., Pytela, R., and Giachelli, C. M. (1996) *J. Biol. Chem.* **271**, 28485–28491
- Liaw, L., Almeida, M., Hart, C. E., Schwartz, S. M., and Giachelli, C. M. (1994) *Circ. Res.* **74**, 214–224
- Fujisawa, R., Mizuno, M., Nodasaka, Y., and Kuboki, Y. (1997) *Matrix Biol.* **16**, 21–28
- Goldberg, H. A., Warner, K. J., Stillman, M. J., and Hunter, G. K. (1996) *Connect. Tissue Res.* **35**, 385–392
- Fujisawa, R., Wada, Y., Nodasaka, Y., and Kuboki, Y. (1996) *Biochim. Biophys. Acta* **1292**, 53–60
- Herzfeld, J. B. (1980) *J. Phys. Chem.* **73**, 6021–6030
- Ruocco, M. J., Siminovitch, D. J., Long, J. R., Das Gupta, S. K., and Griffin, R. G. (1996) *Biophys. J.* **71**, 1776–1788
- Lieske, J. C., Leonard, R., and Toback, F. G. (1995) *Am. J. Physiol.* **268**, F604–F612